

**United States  
Department of  
Agriculture**

**Natural Resources  
Conservation  
Service**

**11 Campus Boulevard,  
Suite 200  
Newtown Square, PA 19073**

**Subject:** SOI – Geophysical Field Assistance

**Date:** 22 April 2004

**To:** Dr. Henry Lin  
Assistant Professor of Hydropedology/Soil Hydrology  
Crop & Soil Sciences Department  
415 Agricultural Sciences and Industries Building  
Pennsylvania State University  
University Park, PA 16802

Edgar White  
State Soil Scientist  
USDA-NRCS  
One Credit Union Place, Suite 340  
Harrisburg, PA 17110-2993

**Purpose:**

Ground-penetrating radar (GPR) and electromagnetic induction (EMI) methods were used to assist the Pennsylvania State University's Hydropedology Team map spatial variations in soils and soil properties within a small watershed.

**Participants:**

Jim Doolittle, Research Soil Scientist, USDA-NRCS-NSSC, Newtown Square, PA  
Henry Lin, Assistant Professor, Crop & Soil Sciences Department, Penn State University, University Park, PA  
Brad Georgic, Senior Research Technologist, Crop & Soil Sciences Department, Penn State University, University Park, PA  
Chip Kogelmann, PhD student, Crop & Soil Sciences Department, Penn State University, University Park, PA  
Ji Zhang, PhD student, Crop & Soil Sciences Department, Penn State University, University Park, PA

**Activities:**

All field activities were completed on 7 to 9 April 2004.

**Summary:**

1. An EMI survey was completed of the watershed with an EM38DD meter operated in the continuous mode with apparent conductivity ( $EC_a$ ) measured at 1-sec intervals. Severe slopes and underbrush impeded progress. In some portions of the watershed, surrounding slopes and vegetation masked reception of GPS signals.
2. Values of  $EC_a$  were comparably low and invariable across most of the watershed, confirming the influence of electrically resistive, acid Rose Hill shale and the pervasiveness of shallow Weikert and moderately deep Berks soils. Apparent conductivity was generally higher in lower-lying, wetter areas that adjoin the major stream, in some swales, and on higher-lying and less sloping summit areas. The accompanying plots of  $EC_a$  are believed to be reflecting changes in clay content and soil depth.
3. Although 2995  $EC_a$  measurements were recorded with the EM38DD meter, data remain sparse and unequally distributed for an area that contains so much perceived variability. Because of the varied topography, the intensity of EMI surveys needs to be greater on steeply sloping and more complex landforms than on more level, simple landforms.

4. Multiple traverses were conducted with the 400 MHz antenna along lines located principally on south-facing slopes of the watershed. In general, observation depths and resolution of subsurface features were adequate for the determination of soil depths. However, because of the nature and complexity of subsurface reflectors, the delineation of soil and bedrock features was extremely challenging and subjective. Though unverified, the accuracy of depth to bedrock measurements was believed to be within  $\pm 25$  cm.
5. Within the watershed, radar records displayed variable structures at all size scales, from centimeters to tens of meters. Changes in reflector characteristics such as shape, continuity, and amplitude can be used to characterize major radar facies. Radar facies represent assemblages or groups of similar radar reflection types. Terminations of radar facies identify bounding surfaces. Though qualitative, radar facies appearing on the accompanying radar records can be used to help characterize general soil patterns within the watershed.
6. Advance processing techniques aid interpretation of radar records. In particular, surface normalization of radar records aids soil/landscape correlations and improves interpretations.
7. In future studies of the Shale Hills Watershed, detailed radar investigations of small selected areas and the construction of 3D imagery may be used to improve knowledge of the variability of soils and soil properties.
8. Bitmap files of all radar records have been forwarded to Brad Georgic under a separate cover letter.

It was my pleasure to participate in this study and to work with the faculty and staff of Pennsylvania State University.

With kind regards,

James A. Doolittle  
 Research Soil Scientist  
 National Soil Survey Center

cc:

B. Ahrens, Director, USDA-USDA-NRCS, National Soil Survey Center, Federal Building, Room 152, 100 Centennial Mall North, Lincoln, NE 68508-3866

S. Carpenter, MLRA Office Leader, USDA-NRCS, 75 High Street, Room 301, Morgantown, WV 26505

M. Golden, Acting Director of Soils Survey Division, USDA-NRCS, Room 4250 South Building, 14th & Independence Ave. SW, Washington, DC 20250

C. Olson, National Leader for Soil Investigations, USDA-USDA, National Soil Survey Center, Federal Building, Room 152, 100 Centennial Mall North, Lincoln, NE 68508-3866

W. Tuttle, Soil Scientist (Geophysical), USDA-NRCS, National Soil Survey Center, P.O. Box 974, Federal Building, Room 206, 207 West Main Street, Wilkesboro, NC 28697

### Shale Hills Watershed:

The Pennsylvania State University's Hydropedology Team is studying spatial and temporal variations in soil properties that influence the distribution and flow of soil water at different scales within the Shale Hills Watershed. The watershed is located near the Stone Valley Recreation Center in Huntingdon County (~15 miles from State College). This forested watershed is relatively small (7.8 ha) and well defined. Figure 1 shows the relative topography of the watershed. This map was prepared from GPS measurements. Based on these measurements, elevations range from 232.5 to 275.8 m within the watershed. In Figure 1, a segmented, blue-colored line has been used to indicate the approximate location of the small stream that drains the watershed. This stream is intermittent along most of its course through the watershed. Within the watershed, a continuous flow of water is maintained throughout the year only along the lower course of the stream. This portion of the stream lies beneath a thick canopy of evergreen trees. Also shown in Figure 1 are the locations of the radar traverse lines (colored either red or yellow) that were conducted during this study.

The watershed has been mapped principally as Berks-Weikert association, steep, and Ernest silt loam, 3 to 8 percent slopes (Merkel, 1978). The watershed also includes small areas of Berks-Weikert shaly silt loam, 15 to 25 percent slopes, and Berks shaly silt loam, 8 to 15 percent slopes (Merkel, 1978). The Pennsylvania State University's Hydropedology Team has completed an order-one soil survey of the watershed. On the high intensity soil map, Weikert soil dominates most of the higher-lying and more sloping plane and convex slopes of the watershed. Earnest and Blairton soils are restricted to the main stream channel. Berks and Rushtown soils have been mapped in swales or shallow ravines form by smaller, contributing intermittent streams. All soils contain large amounts of rock fragments and have varying depths to thinly bedded and highly fractured bedrock. Within the watershed, the underlying bedrock is Rose Hill shale.

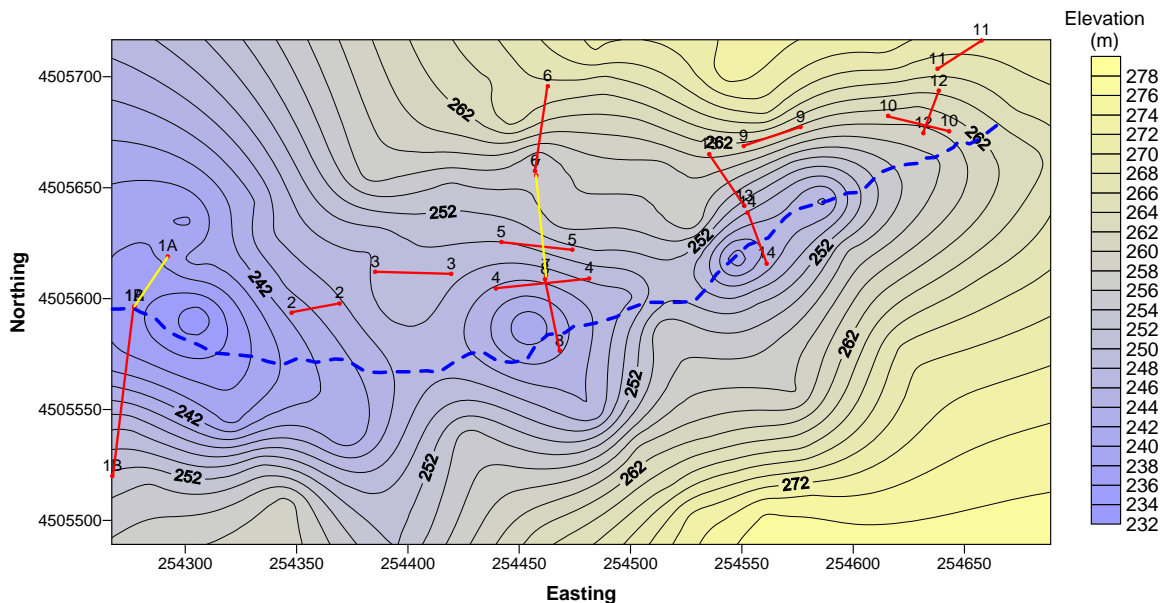


Figure 1. Relative topography of the Shale Hills Watershed (Based on GPS measurements).

All soils formed in materials weathered from shale. The well drained, shallow Weikert and moderately deep Berks soils are on gently sloping to very steep slopes. Weikert is a member of the loamy-skeletal, mixed, active, mesic Lithic Dystrudepts family. Depths to bedrock ranges from 25 to 50 cm in Weikert soil. The Berks soil is a member of the loamy-skeletal, mixed, active, mesic Typic Dystrudepts family. The moderately deep, somewhat poorly drained and moderately well drained Blairton soil is on swales and drainage heads. Blairton is a member of the fine-loamy, mixed, active, mesic Aquic Hapludults family. For Berks and Blairton soils, depths to bedrock range from 50 to 100 cm.

The very deep, moderately well drained Ernest soil is on foot slopes. Ernest is a member of the fine-loamy, mixed, superactive, mesic Aquic Fragiudults family. A fragipan is within depths of about 50 to 90 cm. The very deep,

excessively drained Rushtown soil is on swales. Rushtown is a member of the loamy-skeletal over fragmental, mixed, active, mesic Typic Dystrudepts family. For Ernest and Rushtown soils, depths to bedrock are greater than 152 cm.

### **Equipment:**

The radar unit is the TerraSIRch Subsurface Interface Radar (SIR) System-3000 (here after referred to as the SIR System-3000), manufactured by Geophysical Survey Systems, Inc.<sup>1</sup> The SIR System-3000 consists of a digital control unit (DC-3000) with keypad, SVGA video screen, and connector panel. A 10.8-volt lithium-ion rechargeable battery powers the system. The SIR System-3000 weighs about 9 lbs (4.1 kg) and is backpack portable. With an antenna, this system requires two people to operate. A 400 MHz antenna was used in this study. The use and operation of GPR are discussed by Morey (1974), Doolittle (1987), and Daniels (1996).

The RADAN for Windows (version 5.0) software program developed by Geophysical Survey Systems, Inc, was used to process the radar records.<sup>1</sup> Processing included setting the initial pulse to time zero, color table and transformation selection, marker editing, distance normalization, range gain adjustments, migration, and surface normalization. All radar records were migrated to remove hyperbola diffractions and to correct the geometry of steeply dipping layers. Surface normalization corrects the radar record for changes in elevation and, in this study, greatly improved interpretations and the association of subsurface reflectors with soils and landscape components.

Geonics Limited manufacturers the EM38DD.<sup>1</sup> The EM38DD meter is portable and requires only one person to operate. No ground contact is required with this meter. Geonics Limited (2000) describes the use and operation of the EM38DD meter. The EM38DD meter consists of two EM38 meters bolted together and electronically coupled. One unit acts as a master unit (meter that is positioned in the vertical dipole orientation and having both transmitter and receiver activated) and one unit acts as a slave unit (meter that is positioned in the horizontal dipole orientation with only the receiver switched on). Each meter has a 1 m intercoil spacing and operates at a frequency of 14,600 Hz. The EM38DD meter has effective penetration depths of about 0.75 and 1.5 m in the horizontal and vertical dipole orientations, respectively (Geonics Limited, 2000).

The Geonics DAS70 Data Acquisition System was used to record and store both EMI and GPS data.<sup>1</sup> The acquisition system consists of an EM38DD meter, Allegro field computer, and Trimble AG114 GPS receiver.<sup>1</sup> With the acquisition system, the EM38DD meter is keypad operated and measurements were automatically triggered.

To help summarize the results of this study, SURFER for Windows (version 8.0) software developed by Golden Software, Inc.,<sup>1</sup> was used to construct two-dimensional simulations. Grids were created using kriging methods with an octant search.

### **Survey Procedures:**

Radar traverses were completed along selected lines established across different landscape components and soil polygons (see Figure 1). These traverse lines were located principally on the south-facing slopes of the watershed. Along each line, reference flags were inserted in the ground at either a regular interval of 1.5 or 3 m. Pulling the 400 MHz antenna along each line completed the GPR survey. Along each line, as the antenna was towed passed a reference point, a vertical mark was impressed on the radar record.

Based on the depth to a known, buried reflector and a hyperbola-matching program in RADAN Windows NT, the velocity of propagation was observed to decrease with increasing depth, but averaged about 0.08 m/ns through the upper part of the soil profile (dielectric permittivity of 12.9). Using this velocity, a scanning time of 60 nanoseconds provided a maximum penetration depth of about 2.5 m.

An EMI survey was completed of the watershed. The EM38DD meter was held about 8 cm above the ground surface with its long axis parallel to the direction of travel. The EM38DD meter was operated in the continuous mode and the DAS 70 Acquisition System recorded a geo-referenced apparent conductivity ( $EC_a$ ) measurement at 1-sec intervals. Walking in a back and forth pattern across the watershed, 2995 geo-referenced  $EC_a$  measurements were recorded. Severe slopes made the work demanding. Underbrush and litter repeatedly blocked the EM38DD meter and ensnarled wires to the DAS70

<sup>1</sup> Manufacturer's names are provided for specific information; use does not constitute endorsement.

acquisition system, thus further impeding progress. The surrounding slopes and vegetation masked reception of GPS signals in some portions of the watershed.

## Results:

### EMI:

Values of apparent conductivity were comparably low and invariable across most of the watershed, confirming the influence of electrically resistive, acid Rose Hill shale and the pervasiveness of shallow Weikert and moderately deep Berks soils. Apparent conductivity was generally higher in lower-lying, wetter areas that adjoin the major stream, in some swales, and on higher-lying and less sloping summit areas.

Table 1 summarizes the results of the April EMI survey of the watershed. At the time of the survey, the soil temperature at a depth of about 50 cm was 46° F. Based on this measurement, all apparent conductivity ( $EC_a$ ) values have been corrected to a standard temperature of 25° C. At the time of this study, soils were moist throughout. Values of  $EC_a$  ranged from about -22 to 26 mS/m. Negative values are attributed to calibration errors and/or surface or near-surface metallic artifacts. With the EM38DD meter,  $EC_a$  was remarkably low in the upper 75cm of soil profiles and generally increased with increasing depth. The known soils and geology of the watershed would indicate that  $EC_a$  should decrease with increasing depth over much of the watershed. The anomalously low  $EC_a$  at shallow depths is attributed to calibration and operating errors.

**Table 1. Basic EMI Statistics for EMI Survey of Shale Hills Watershed  
April 2004**

	EM38DD-V	EM38DD-H
<b>Number</b>	2995	2995
<b>Minimum</b>	-22.4	-0.1
<b>Maximum</b>	25.8	20.0
<b>25 % Percentile</b>	7.2	4.3
<b>75 % Percentile</b>	11.4	7.5
<b>Mean</b>	9.3	6.0
<b>SD</b>	3.0	2.6

In the shallower-sensing, horizontal dipole orientation (0 to 0.75 m depth),  $EC_a$  averaged about 6.0 mS/m with a standard deviation of about 2.6 mS/m (see Table 1). One-half the observations had values of  $EC_a$  between 4.3 and 7.5 mS/m. In the deeper-sensing, vertical dipole orientation (0 to 1.5 m depth),  $EC_a$  averaged about 9.3 mS/m with a standard deviation of about 3.0 mS/m. One-half the observations had values of  $EC_a$  between 7.2 and 11.4 mS/m. The higher  $EC_a$  at deeper depths can be attributed to greater moisture contents at lower soil depths and the sensitivity of horizontal dipole measurements to the thin air column (about 7 cm) that separates the meter from the ground surface.

Figure 2 contains contour plots of  $EC_a$  measured with the EM38DD meter. The upper plot shows the spatial distribution of  $EC_a$  measured in the shallower-sensing horizontal dipole orientation. The lower plot shows the spatial distribution of  $EC_a$  measured in the deeper-sensing, vertical dipole orientation. Color variations have been used to show the distribution of  $EC_a$ . In each plot, the color interval is 3 mS/m. Throughout most of the watershed,  $EC_a$  is low and invariable reflecting the dominance of the Berks and Weikert soils and the control of the underlying Rose Hill shale. In each plot, higher values of apparent conductivity can be observed along the lower course of the stream channel, especially where it departs the western side of the watershed.

Values of  $EC_a$  are comparatively low and invariable within the watershed. However, spatial patterns appear highly complicated. Although  $EC_a$  increases with increasing moisture content, the effect of changes in moisture content on  $EC_a$  is less apparent as the water content increases above field capacity (Auerswald et al., 2001). At these moisture contents, the affects of changes in clay contents on  $EC_a$  are more significant. Therefore, the plots of apparent conductivity shown in Figure 2 are believed to be reflecting changes in clay content and soil depth.

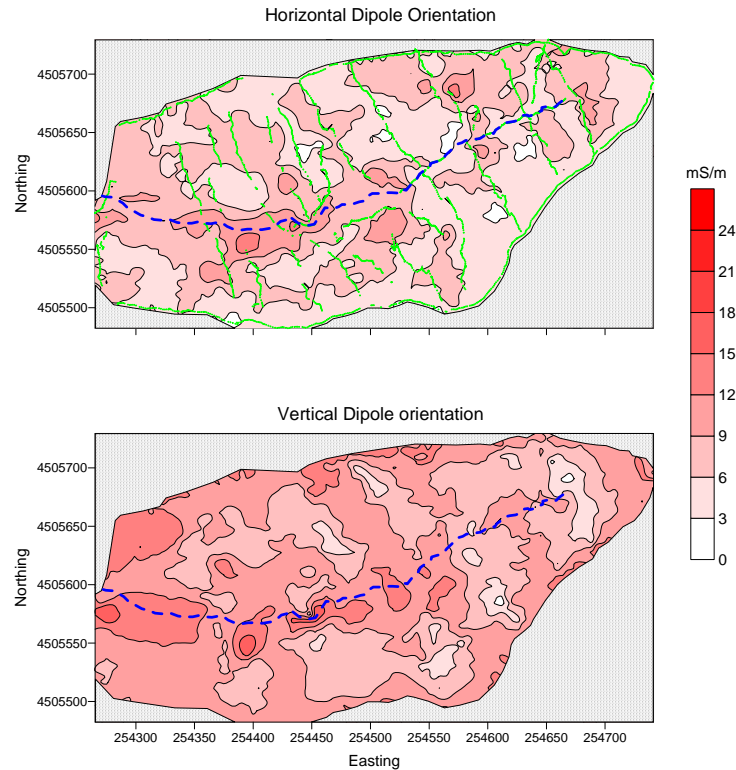


Figure 2. Plots of  $EC_a$  data collected with the EM38DD meter within the Shale Hills Watershed.

Because of the steep, forest terrain, it is not easy to complete an EMI survey of the watershed. The location of the 2995 observations recorded with the EM38DD meter are shown (green-colored dots) in the upper plot of Figure 2. At first glance, most of the watershed appears equally sampled. However, landscapes and soil patterns are highly variable and many slope components were not sampled and observable soil and landscape boundaries were not sufficiently delineated with EMI. Data remain sparse and unequally distributed for an area that contains so much perceived variability. Because of the varied topography, the intensity of EMI surveys needs to be greater on steeply sloping and more complex landforms than on more level, simple landforms.

This survey was conducted when trees were mostly free of a leaf canopy. The western portion of the watershed is covered with evergreen trees that limit GPS reception and the plotting of  $EC_a$ . In other portions of the watershed, the boles of larger trees and steep slopes restricted the visibility of satellites. As a consequence, gaps can be seen in the spacing of observation points along traverse lines. During summer months, the visibility of satellites will be even more restricted and a similar sampling scheme will result in sparser data.

#### GPR Survey:

Multiple traverses were conducted with the 400 MHz antenna along lines located principally on south-facing slopes of the watershed. In general, observation depths and resolution of subsurface features were adequate for the determination of soil depths. However, because of the nature and complexity of subsurface reflectors, the delineation of soil and bedrock features was extremely challenging and subjective.

Figure 4 is a radar record of a 21-m section from a traverse conducted in an area of Berks soil. The radar traverse was conducted orthogonal to the long axis of a shallow ravine or swale that was located in the western portion of the watershed (see line 2 in Figure 1). All scales on this radar record are in meters. In Figure 4, a green-colored line has been used to identify the soil/bedrock interface; a blue-colored line has been used to identify a subsurface soil horizon or layer of colluvium.

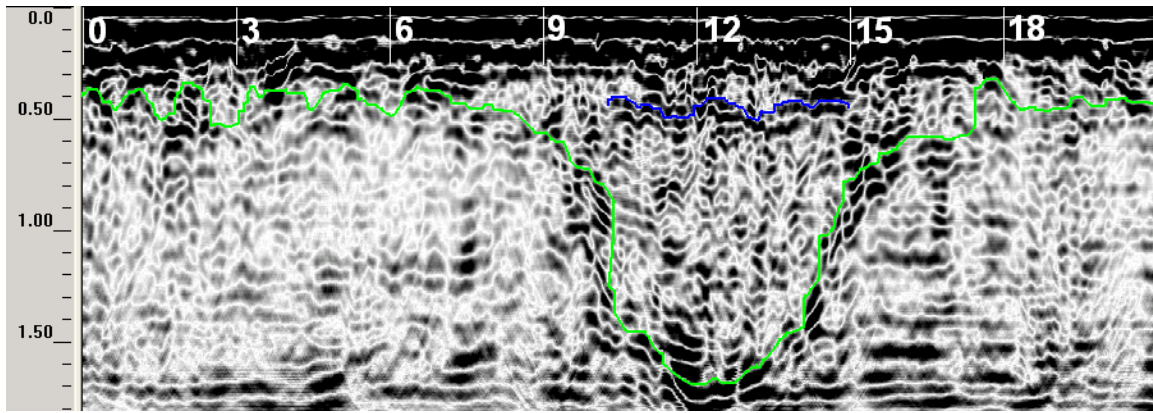


Figure 4. Depth to bedrock and soil layers are charted on this distant normalized radar record from a swale of Berks soil.

No subsurface reflectors were evident on radar records below the soil/bedrock interface. In place, clustering of point reflectors and hyperbola suggests areas of intense or wider fracturing in the underlying bedrock. However, on most radar records, other than parallel bands of noise, the underlying shale bedrock was remarkably free of subsurface reflections. The absence of subsurface interfaces was used to help identify the shale bedrock. Assemblages or groups of similar radar reflection types (chaotic, high-angle clinofolds, parallel/planar, sigmoidal, and hummocky/wavy) are known as radar *facies*. Terminations of *radar facies* identify bounding surfaces that indicate erosional unconformities. In Figure 4, shallow soils consist of a sequence of parallel, planar surface reflections immediately underlain by discontinuous, hummocky planar reflectors. In the central portion of Figure 4, chaotic reflectors of various forms indicate an area of unconsolidated fill materials. The absence of reflections indicates the shale bedrock. Though qualitative, these three radar facies can be used to help characterize the radar record.

In Figure 4, a green-colored line has been used to identify the approximate location of the soil/bedrock interface. The appearance of this interface is highly irregular, segmented, and variable in amplitude. As a consequence, the soil/bedrock interface is exceedingly difficult to consistently and unambiguously delineate on the radar records. Because of the lack of a lone, well expressed, continuous, high-amplitude reflection, the picking of the soil/bedrock interface was unclear and the accuracy of interpreted soil depth measurements is lessened. While the picking of the soil/bedrock interface is problematic, the lines shown in this report are considered accurate to within  $\pm 10$  to 25 cm of the true depth.

General trends are evident in Figure 4. Soil depths are dominantly shallow between reference points 0 and 6 m and 15 and 21 m. Soil depths are deeper between reference points 6 and 15 m. Reference points 6 to 15 are located within a swale that has been mapped as Berks soil. Interpreting the soil depth at 50 cm intervals (laterally along traverse line) within the bowl shaped feature that is evident in Figure 4 between reference points 6 and 15, the average depth is 88.96 cm with a range of 26 to 170 cm. One half the observations ( $n = 25$ ) have depths between 49 and 142 cm. Within this swale, soils are shallow at 32 %, moderately deep at 32 %, deep at 16%, and very deep at 20% of the 25 measurement points.

Through a process known as “surface normalization” elevations are assigned to each reference point and radar records can be corrected for changes in elevation. Surface normalization more accurately displays the topography of subsurface reflectors. Figure 5 is a surface normalized representation of the radar record shown in Figure 4. A color table of 1 and a color transformation of 4 has been used in Figure 5. All units of measure are expressed in meters. Because the relative change in topography is greater than the display range of the monitor, the vertical scale has been compressed (by a factor of 4). Once again, a green-colored line has been used to approximate the interpreted depth to bedrock.

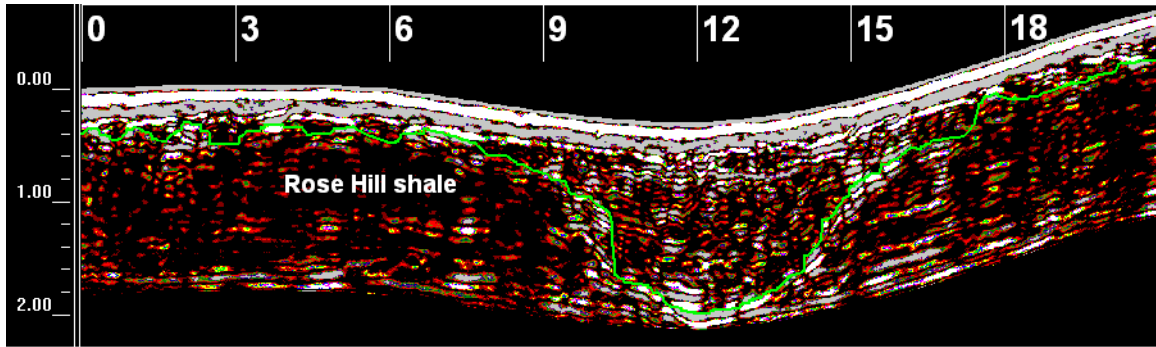


Figure 5. Depth to bedrock and soil layers are charted on this surface normalized radar record from a swale of Berks soil.

The surface normalized presentation in Figure 5 aids soil/landscape correlations and improves interpretations. Soils are conspicuously deeper in the shallow ravine or swale that has been mapped as Berks soil. The ravine appears to have been scoured to bedrock and then filled with unconsolidated soil materials and rock fragments. In this cross-sectional view, which is orientated orthogonal to the ravine's long axis, alternating, horizontal layers are apparent within the unconsolidated fill materials. In Figure 5, the radar record confirms the dominance of moderately deep and deep soils in the shallow ravine. Along this traverse, deep and very deep soils are equal in extent to the recognized moderately deep Berks soil. Soils are shallow on the upper side slopes that descend into the ravine. Here, soils were mapped as Weikert.

Figure 6 is a bitmap image of the radar record from line 4 (see Figure 1). This traverse line is 75 m long and orthogonal to the long axis of a wider swale. This swale has been mapped as associations of Berks and Rushtown soils. In Figure 6, the depth scale is in meters. The radar record has been surface normalized. The vertical scale has been compressed (by a factor of 4). The short vertical marks at the top of the radar record are equally-spaced (3 m) reference points.

In Figure 6, a dark-colored line has been used to approximate the interpreted depth to bedrock. At each end of this radar record, shallow Weikert soil dominates the higher-lying and less sloping areas. A very narrow band of moderately deep Berks soils is on the upper side slopes into the swale. Deep and very deep soils dominate the central portion of this swale. This area had been mapped as Rushtown soil. Once again, a deeper ravine appears to have been scoured to bedrock and then filled with unconsolidated materials. The radar record shows multiple, near-horizontal reflectors in the unconsolidated fill materials. These reflectors are presumed to represent contrasting layers of fill materials that influence the flow of soil water.

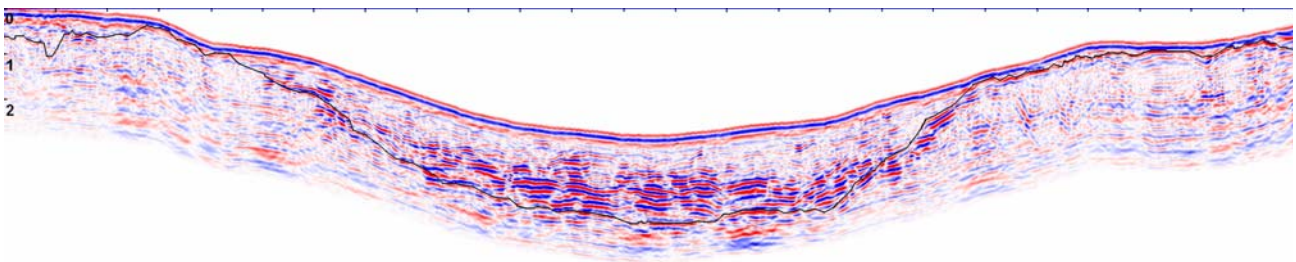


Figure 6. Depth to bedrock and soil layers are charted on this surface normalized radar record from a wider swale that contains areas of Berks and Rushtown soils.

The radar record shown in Figure 6 is 75 m long. This length is too excessive to be suitably displayed in RADAN for Windows or as a bitmap file. To permit display, the image has been significantly compressed and reduced making features difficult to distinguish. Although general soil-depth and stratigraphic trends are illustrated, the scale of this figure does not permit the adequate expression of many smaller and more variable soil features, many of which are poorly expressed.

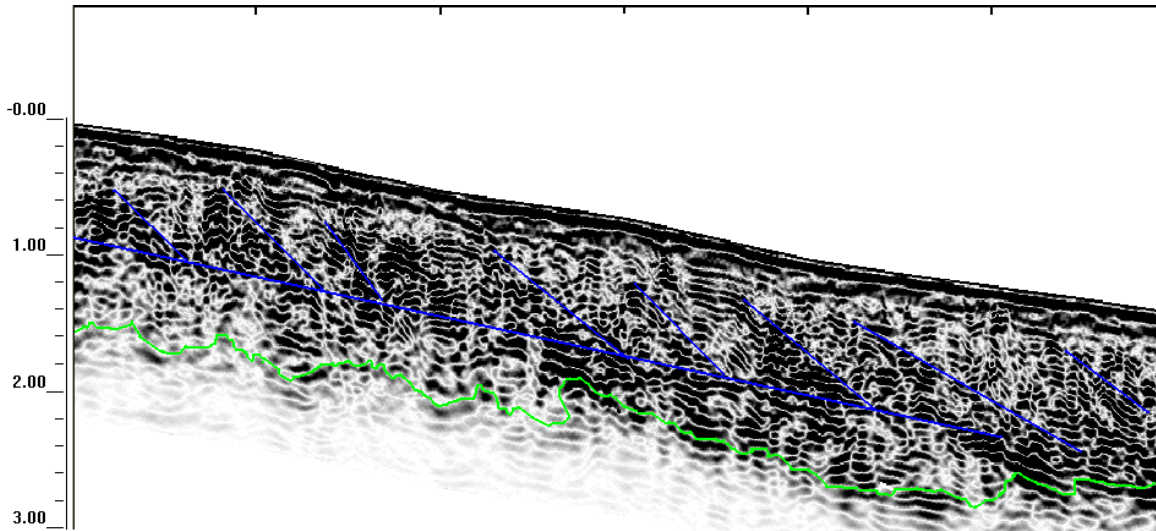


Figure 7. A surface normalized radar record from a traverse conducted parallel with the long axis of a wider swale that contains mapped areas of Berks and Rushtown soils.

Figure 7 shows an 18-m section of traverse line 6 (see Figure 1). This traverse was conducted on a drainage head, along the center axis of the large swale whose cross-section is shown in Figure 6. Color table 19 with a display gain of 4 has been applied to this radar record. The radar record shown in Figure 7 has been surface normalized. The depth scale is in meters. The short, black, vertical lines at the top of the radar record represent equally-spaced (3 m) reference points.

The radar imagery in Figure 7 is very intricate and difficult to comprehend. The muddles of segmented subsurface interfaces are difficult to follow, accurately trace, and identify. A green-colored line has been used to identify the interpreted bedrock surface. The unconsolidated fill material contains a large number of rock fragments that often increases and grades with depth into shale bedrock. The soil/bedrock interface is neither well expressed nor easy to identify on this radar record. The absence of subsurface reflectors has been used to identify the Rose Hill formation on this and other radar records. The lowest recognizable planar reflector has been used as the bedrock surface. While this reasoning has not been confirmed with ground-truth core observations, it provides a criterion for interpretations.

The radar record shown in Figure 7 is from the long axis of a large swale. Several inclined masses of high amplitude reflectors are evident within the fill materials on this record. As these masses or beds dip from slight to steep angles in a down slope direction, their orientation suggest successive flowage of earthen materials. These alternating layers of fill material undoubtedly vary in composition, density, and permeability. The reflection patterns suggest a sequence of heterogeneous masses composed of soil materials and rock fragments that were deposited in seemingly catastrophic flowage cycles.

Figure 7 (and most of the other radar records contained in this report) can be interpreted using radar facies. A radar facies is defined as a “mappable three-dimensional sedimentary unit composed of reflections whose parameters differ from adjacent units” (Jol and Smith, 1991). Parameters used in interpretations include the amplitude, continuity, and configuration of radar reflections. In radar facies analysis a portion of a radar profile that has a unique and identifiable graphic signature (a distinct, aggregate configuration, appearance, or pattern) is used to identify a stratigraphic units composed of like materials and distinguishable sedimentary structure or geometry.

Three distinct radar facies are evident in Figure 7. The upper-most facies consists of complex, discontinuous, parallel reflectors that dip from slight to steep angles. These reflectors have high signal amplitudes suggesting strong dielectric gradients across interfaces. The middle facies appears as rather broken and wavy reflector that parallels the ground

surface. This may be a saturated zone at the base of the fill. The lower-most interface is the irregular, discontinuous, and generally low amplitude reflector assumed to be the soil/bedrock interface.

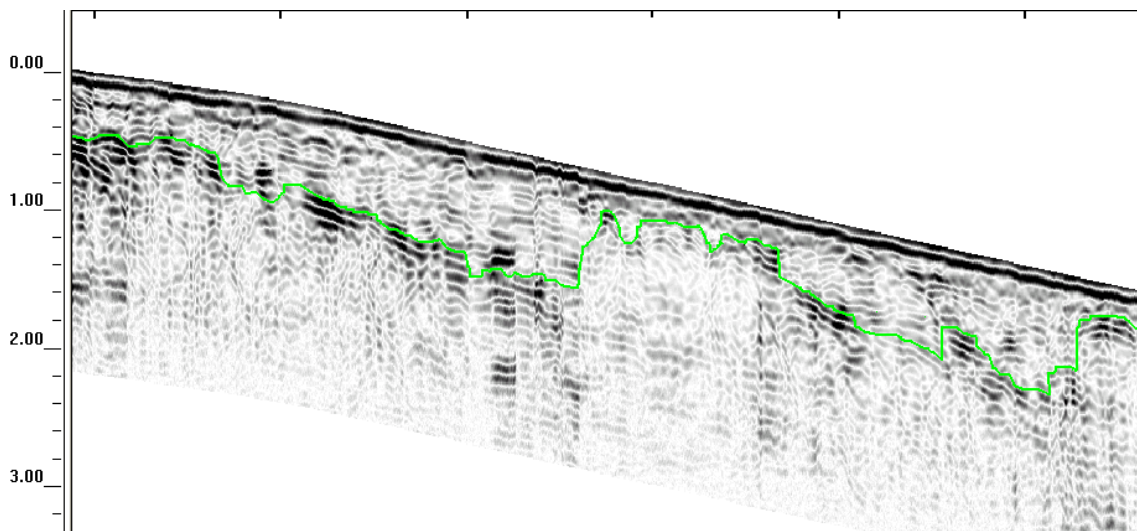


Figure 8. A surface normalized radar record from a traverse conducted across a convex shoulder slope in an area of Weikert soil.

Figure 8 shows an 18-m section of traverse line 13 (see Figure 1). The portion of the radar traverse shown in Figure 8 was conducted across a convex linear shoulder slope in an area mapped as Weikert soil. The radar record shown in Figure 8 has been surface normalized. The depth scale is in meters. The short, black, vertical lines at the top of the radar record represent equally-spaced (3 m) reference points. Color table 19 with a display gain of 2 has been applied to this radar record.

In Figure 8, a green-colored line has been used to show the interpreted soil/bedrock interface. General trends are evident in Figure 8. Interpreting the soil depth at 1 m intervals along this section, the average depth to bedrock is 0.55 m with a range of 28 to 95 cm. One half the observations ( $n = 19$ ) have depths between 35 and 68 cm. Along this shoulder slope, soils are shallow at 42 % and moderately deep at 58 % of the 19 measurement points. Though mapped as Weikert soil, significant areas along this slope segment are Berks soil.

### 3D images:

As done in this study, the form and geometry of subsurface features can be studied in detail from two-dimensional, intersecting radar profiles (van Heteren et al., 1998). Recently, with the advent of digital GPR outputs and advanced data processing software, it has become possible to analyze the structure or configuration of subsurface features from a three-dimensional perspective. Under favorable conditions, GPR and 3D imaging can provide additional information and perspectives of the subsurface. In order to better understand the structure or configuration of many subsurface features, a series of parallel radar records are obtained over soil, lithologic, and/or stratigraphic features. Three-dimensional images allow the rapid display of the data volume from different cross-sections and directions (Beres et al., 1999). However, the acquisition of data for 3D images requires greater resources than the collection of 2D radar records. To construct 3D images, a relatively small area is intensively surveyed with closely spaced (often <1 m), parallel GPR traverses. Data from these lines are processed into a 3D image. Once processed, arbitrary cross-sections, insets, and time slices can be extracted from the 3D data set. The flexibility of 3D visualizations can facilitate the interpretation of spatial relationships and the analysis of soil, structural, and/or stratigraphic features. This imaging technique enables views of the subsurface from nearly any perspective (Junck and Jol, 2000). Detailed radar investigations of small selected areas and the construction of 3D imagery may improve our knowledge of the variability of soils and soil properties within the Shale Hills Watershed.

## References:

- Auerswald, K., S. Simon, and H. Stanjek. 2001. Influence of soil properties on electrical conductivity under humid water regimes. *Soil Science* 166(6): 382-390.
- Beres, M., P. Huggenberger, A. G. Green, and H. Horstmeyer. 1999. Using two- and three-dimensional georadar methods to characterize glaciofluvial architecture. *Sedimentary Geology*, 129: 1-24.
- Daniels, D. J. 1996. *Surface-Penetrating Radar*. The Institute of Electrical Engineers, London, United Kingdom.
- Doolittle, J. A. 1987. Using ground-penetrating radar to increase the quality and efficiency of soil surveys. 11-32 pp. In: Reybold, W. U. and G. W. Peterson (eds.) *Soil Survey Techniques*, Soil Science Society of America. Special Publication No. 20.
- Geonics Limited. 2000. EM38DD ground conductivity meter: Dual dipole version operating manual. Geonics Ltd., Mississauga, Ontario.
- Jol, H. M. and D. G. Smith. 1991. Ground penetrating radar of northern lacustrine deltas. *Can. J. Earth Science*. 28: 1939-1947.
- Junck, M. B. and H. M. Jol. 2000. Three-dimensional investigation of geomorphic environments using ground penetrating radar. 314-318 pp. IN: (Noon, D. ed.) *Proceedings Eight International Conference on Ground-Penetrating Radar*. May 23 to 26, 2000, Gold Coast, Queensland, Australia. The University of Queensland.
- Merkel, E. 1978. *Soil Survey of Huntingdon County, Pennsylvania*. USDA-Soil Conservation Service in cooperation with Pennsylvania State University College of Agriculture and the Pennsylvania Department of Environmental Resources and State Conservation Commission. Government Printing Office, Washington DC.
- Morey, R. M. 1974. Continuous subsurface profiling by impulse radar. p. 212-232. *IN: Proceedings, ASCE Engineering Foundation Conference on Subsurface Exploration for Underground Excavations and Heavy Construction*, held at Henniker, New Hampshire. Aug. 11-16, 1974.
- van Heteren, S., D. M. Fitzgerald, P. A. McKinlay, and I. V. Buynevich. 1998. Radar facies of paraglacial barrier systems: coastal New England, USA. *Sedimentology*, 43: 181-200.